Supporting Information

Rapid Fabrication of Silver Microplates under an Oxidative Etching Environment Consisting of O_2/Cl^-, NH_4OH/H_2O_2, and H_2O_2

*Harnchana Gatemala, Prompong Pienpinijtham, Chuchaat Thammacharoen, Sanong Ekgasit**

Sensor Research Unit, Department of Chemistry, Faculty of Science, Chulalongkorn University 254 Phyathai Road, Patumwan, Bangkok 10330, Thailand

E-mail: sanong.e@chula.ac.th

Keywords: Silver Microplate, Hydrogen Peroxide, Selective Etching, Surface Passivation, Silver Ammine Complex

The chemical reactions in the synthesis of silver microplates (AgMPls) under an oxidative etching environment of O_2/Cl^-, NH_4OH/H_2O_2, and H_2O_2 with H_2O_2 as a sole reducing agent include:

- The formation of $[Ag(NH_3)_2]^+$ complex

$$Ag^+ + 2NH_4OH \rightleftharpoons [Ag(NH_3)_2]^+ + 2H_2O \quad (1)$$

$$AgCl + 2NH_4OH \rightleftharpoons [Ag(NH_3)_2]^+ + Cl^- + 2H_2O \quad (2)$$

- The reduction reaction

$$Ag^+ + e^- \longrightarrow Ag \quad ; E^0 = 0.799\ V \quad (3)$$

$$[Ag(NH_3)_2]^+ + e^- \longrightarrow Ag + 2NH_3 \quad ; E^0 = 0.373\ V \quad (4)$$

- The oxidation reaction

$$H_2O_2 + 2OH^- \longrightarrow 2H_2O + O_2 + 2e^- \quad ; E^0 = 0.146\ V \quad (5)$$

- The redox reaction

$$2[Ag(NH_3)_2]^+ + H_2O_2 \longrightarrow 2Ag + 4NH_3 + 2H_2O + O_2 \quad ; E^0_{cell} = 0.227\ V \qquad (6)$$

- Decomposition of H_2O_2

$$2H_2O_2 \xrightarrow{Ag} 2H_2O + O_2 \qquad (7)$$

- Oxidative etching of metallic silver

$$2Ag + H_2O_2 \longrightarrow 2Ag^+ + 2OH^- \qquad (8)$$

$$Ag + O_2 + Cl^- + 4H^+ \longrightarrow AgCl + 2H_2O \qquad (9)$$

$$2Ag + 4NH_3 + H_2O_2 \longrightarrow 2[Ag(NH_3)_2]^+ + 2OH^- \qquad (10)$$

According to the above equations, the co-existences of H_2O_2, Cl^-, NH_4OH, and the *in-situ* generated O_2 gas made the reaction medium an efficient oxidant for metallic silver. The etchants consisting of H_2O_2,[1] O_2/Cl^-,[2-5] and NH_4OH/H_2O_2[6, 7] are known to oxidatively dissolve metallic silver to silver ion. However, the passivation of Ag{111} by NH_3,[8] Cl^-,[9-13] and AgCl,[13-15] enabled the survival of plate structure in such an oxidative environment.

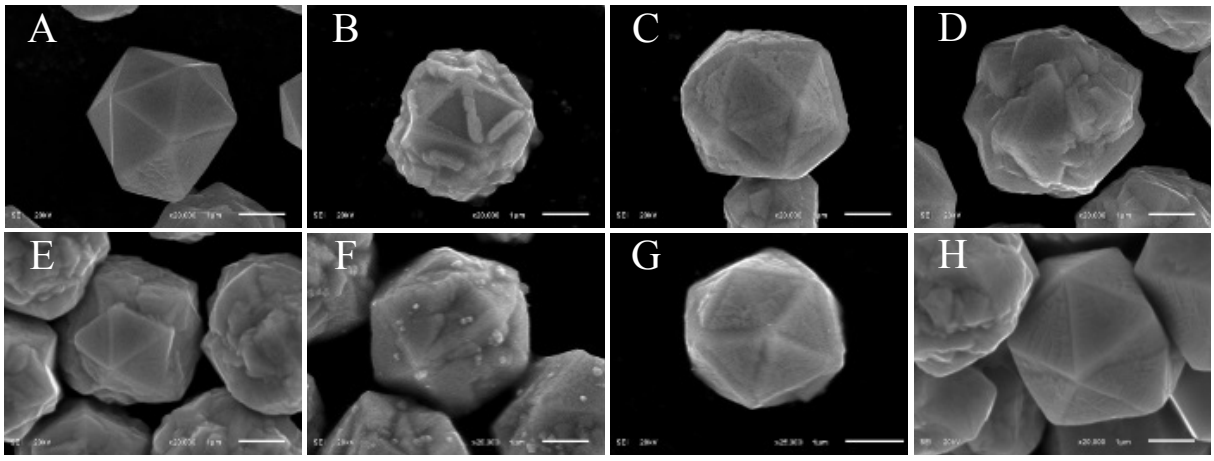

Figure S1. SEM micrographs show the structural evolution of icosahedra under H_2O_2-reduction of $[Ag(NH_3)_2]^+$ complex without Cl^-. The irregular shapes of silver microstructures are, in fact, the under devoloped icosahedra. The above SEM micrographs suggest that the structure grows layer-by-layer.

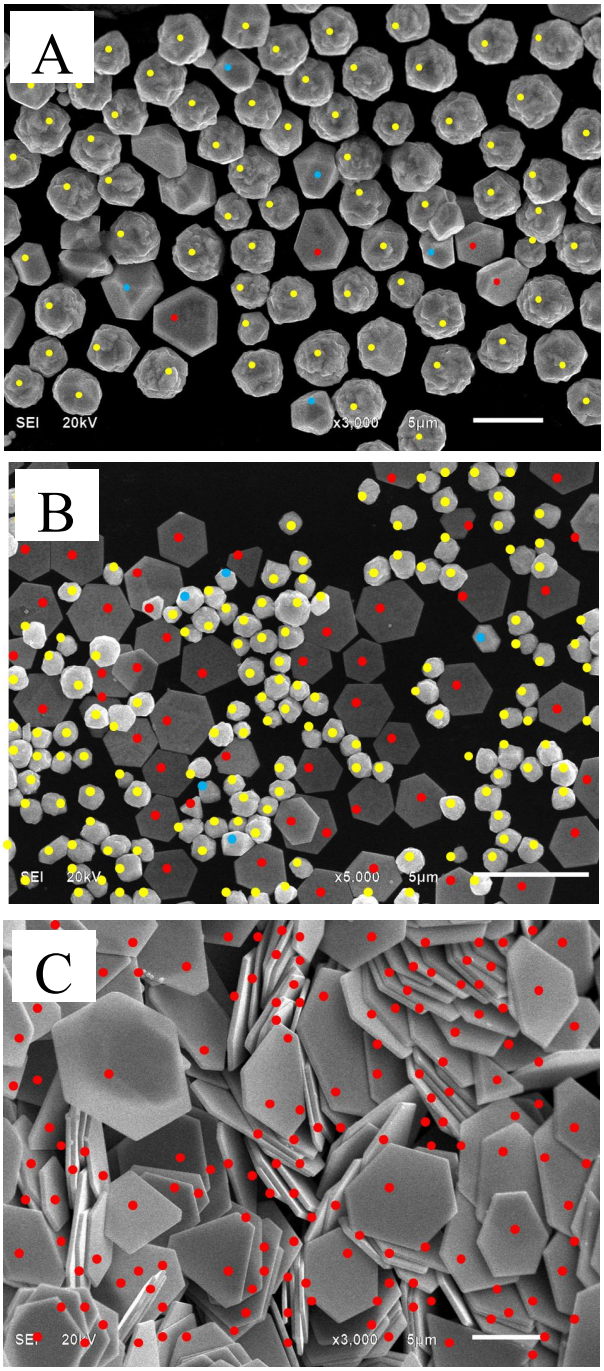

Figure S2. SEM micrographs of silver microparticles synthesized with Cl^- concentration of: (A) 0 mM, (B) 0.05 mM, and (C) 4 mM. The experimental condition are $[AgNO_3]$ = 10 mM, $[H_2O_2]$ = 220 mM, $[NH_4OH]$ = 90 mM, [PVP] = 0.5% w/v. The number average of the structures were calculated from more than 500 particles of unique SEM micrographs. The colours represent: yellow = multiply twinned particles, blue = single crystal particles, and red = plates.

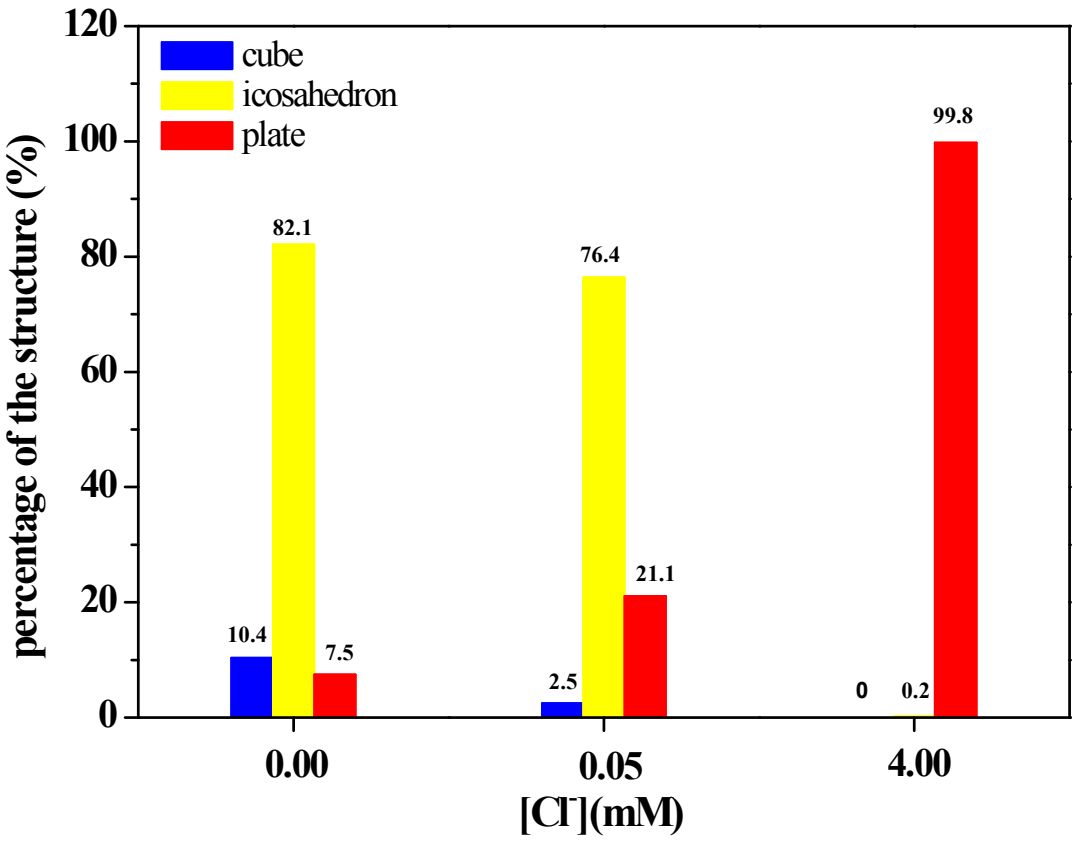

Figure S3. Percentage of cubic, icosahedral, and microplate silver crystals in synthetic conditions shown in Figure 2. The results indicated that Cl^- played an important role as a structural controlling agent as it selectively destroys structure with Ag{100} facet (i.e., cube, icosahedron) while preserves those with Ag{111} (i.e., plate). At Cl^- concentrations greater than 4 mM, the survived population was plate-structures while cubes and icosahedra were disappeared.

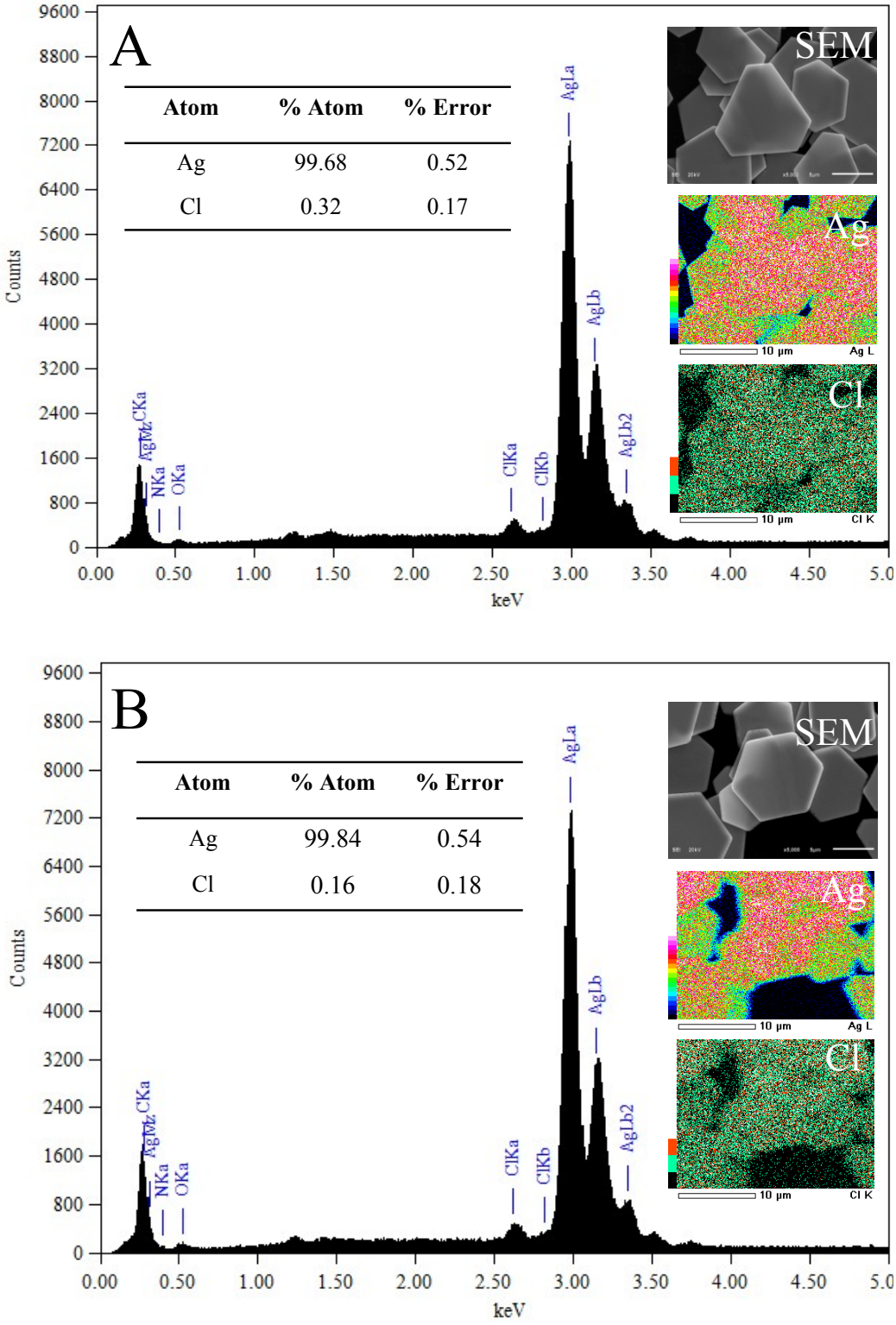

Figure S4. EDS spectra of AgMPls (A) before and (B) after washing with 0.1 M NH_4OH solution. The disappearance of chlorine after washing confirmed the presence of AgCl layer on the surface of as-synthesized AgMPls.

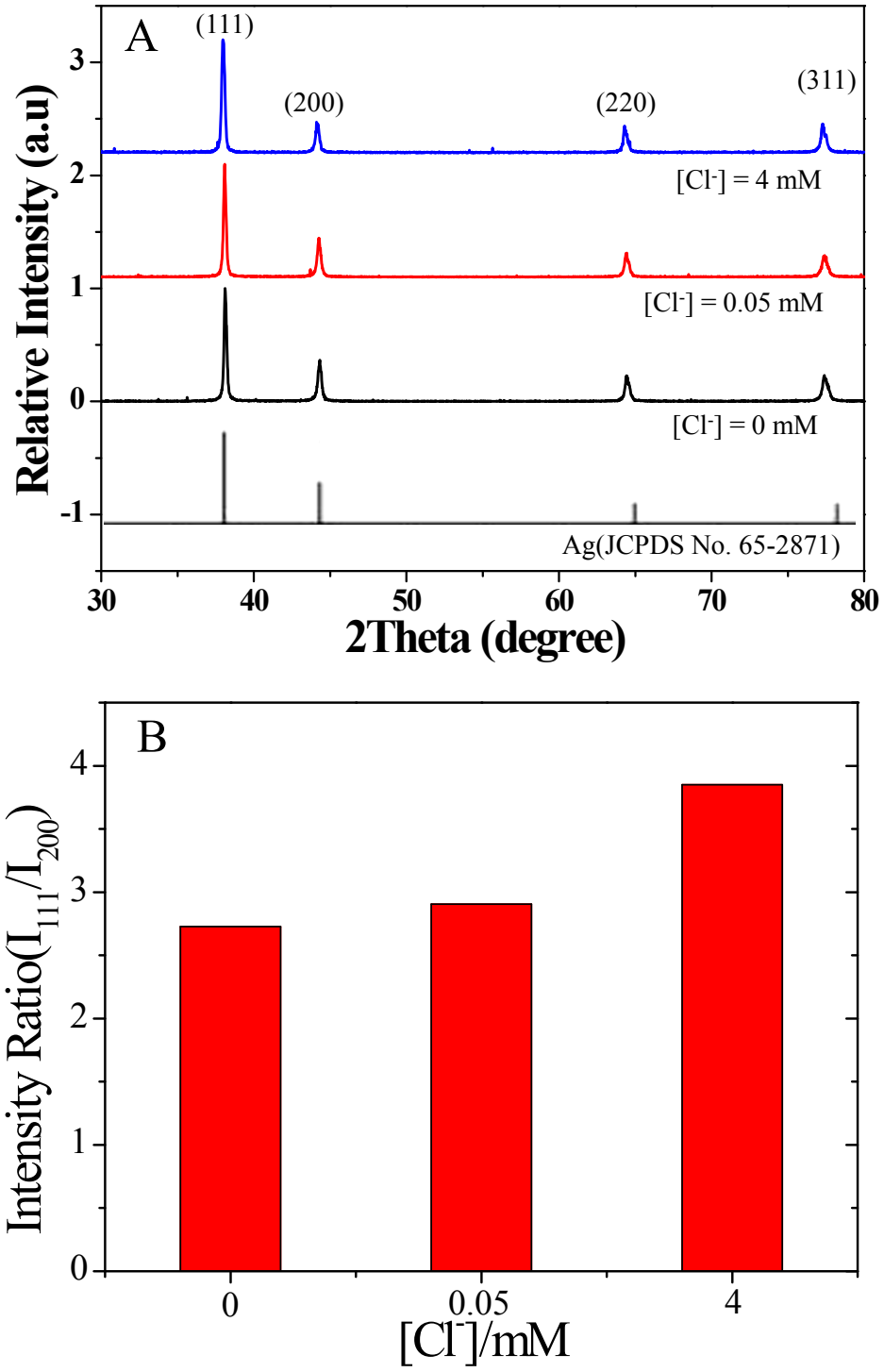

Figure S5. (A) XRD patterns of AgMPs synthesized with different Cl^- concentrations shown in Figure S2. (B) The plot of intensity ratios of (111) and (200) peaks indicates an increment of plate structure with $[Cl^-]$. All patterns correspond to fcc crystal of silver metal (JCPDS No.65-2871).

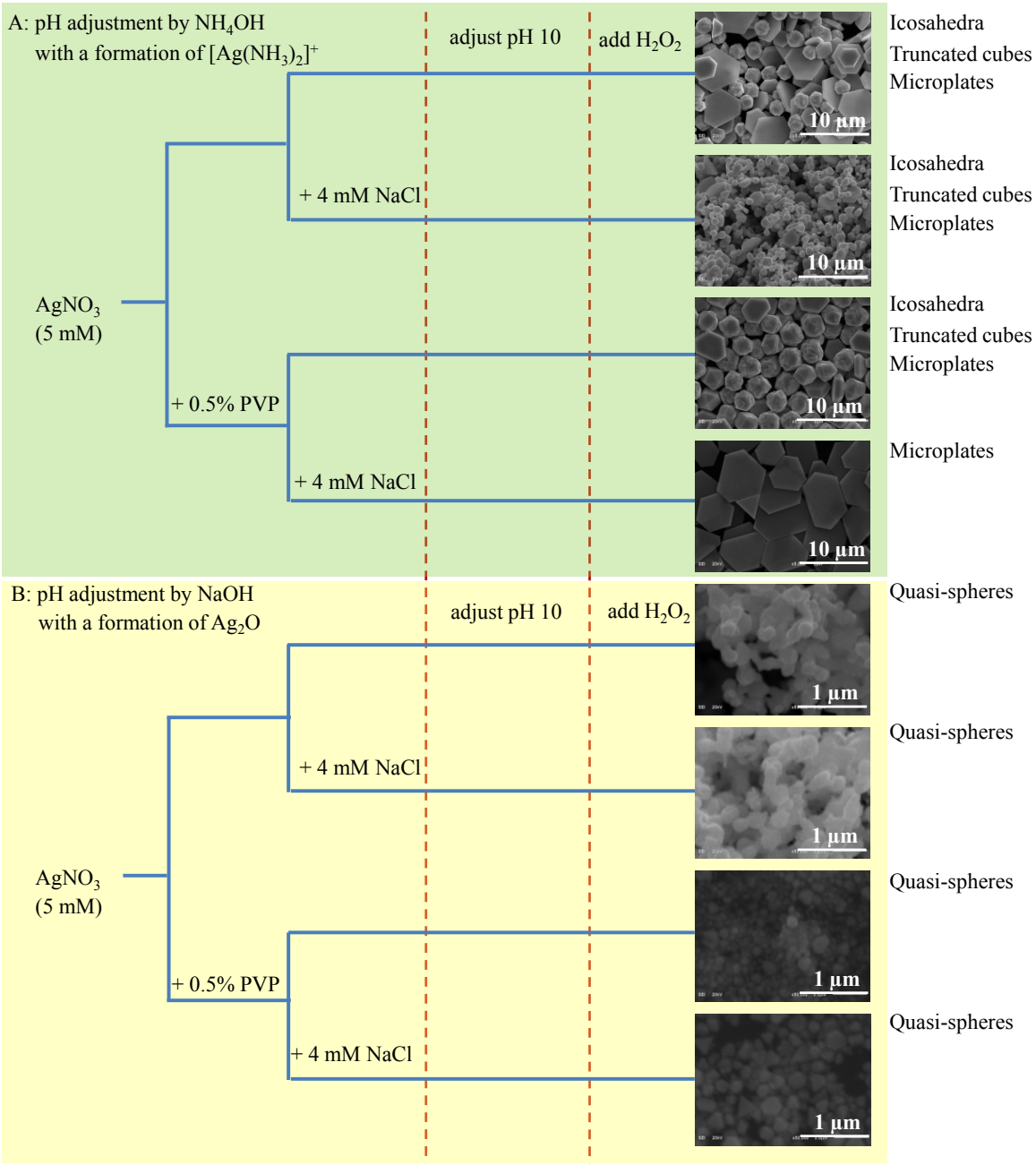

Figure S6. Influences of reaction media on the formation of silver micro/nanostructures under alkaline-H_2O_2 (pH 10) induced by (A) NH_4OH and (B) NaOH. The obtained silver micro/nanostructures suggested that the presence of Cl^- and NH_4OH is crucial for the development of plate structure. PVP is an efficient stabilizer preventing the aggregation while assisting the formation of large silver microstructures.

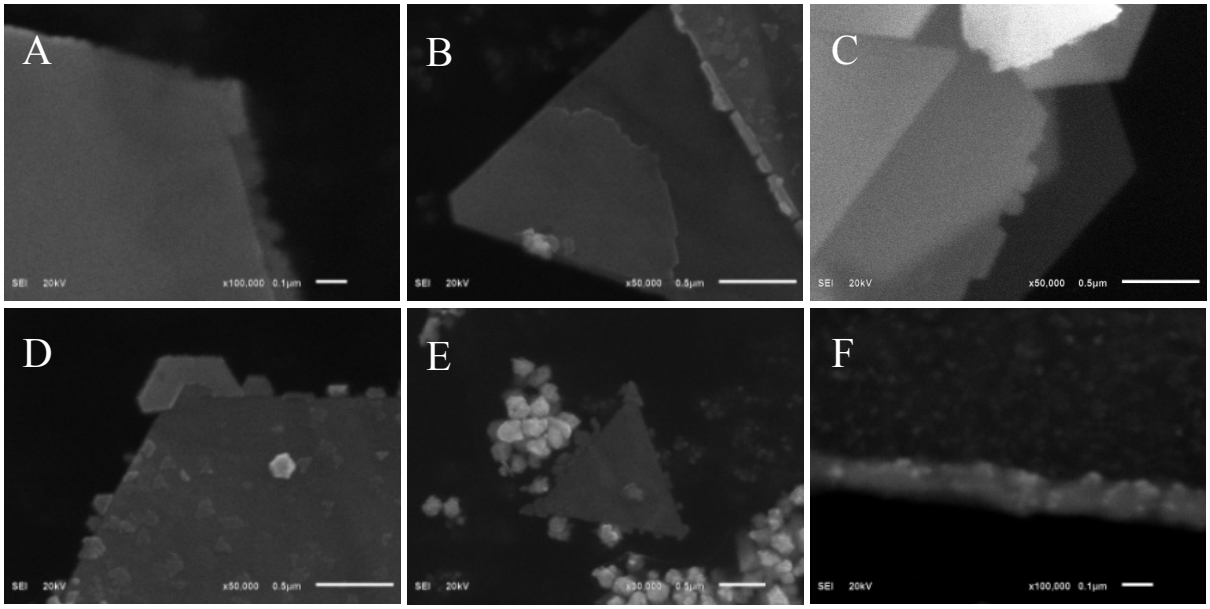

Figure S7. SEM micrographs show evidences of the lateral growth of AgMPls.

According to the experimentally observed phenomena, the following growth mechanism was proposed for the AgMPls. The newly formed silver nnanoplates was bound by basal Ag{111} planes while the alternated Ag{111} and Ag{100} facets covered the lateral sides.[16] Thin layer of AgCl,[13-15] NH_3,[8] and Cl^-[9-13] were selectively adsorbed and passivated the Ag{111} facets. Therefore, Ag{100} facets grew faster than Ag{111} facets (Figures S7A and S7C). An anisotropic growth due to a faster expansion of lateral Ag{100} compared to that of lateral Ag{111} induces a cyclic structural transformation of triangular, truncated triangular, and hexagonal structures during the particle growth process.

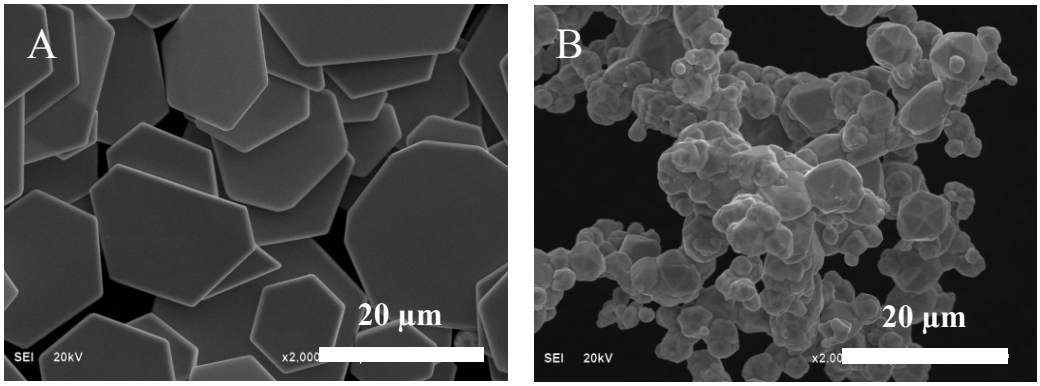

Figure 8. SEM micrographs show AgMPls and AgMPs recovered from wasted AgCl using the developed method: (A) with PVP of 0.5% w/v and (B) without PVP. The recovery conditions were [AgCl] = 10 mM, [H_2O_2] = 220 mM, and [NH_4OH] = 0.18 M. Scale bare indicate 20 µm.

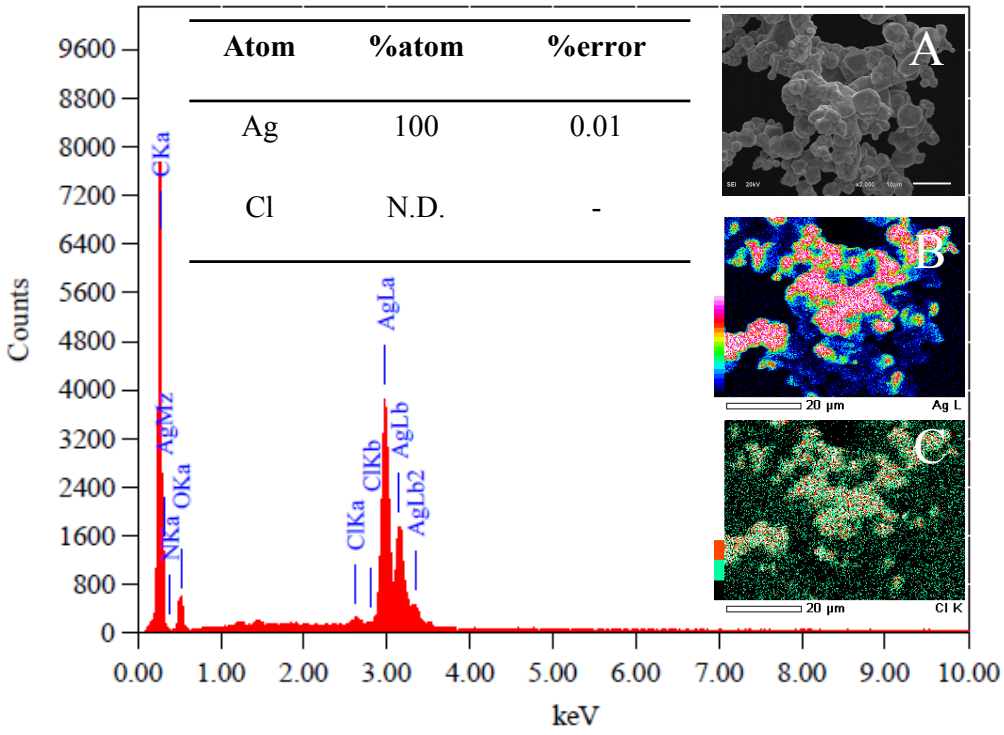

Figure S9. EDS spectrum of AgMPs recovered from waste AgCl using our developed protocol (A) SEM micrograph (B) silver map and (C) chloride map. By rinsing the AgMPs several times with 0.1 M NH_4OH solution, the residual AgCl on the surface can be completely removed, as suggested by EDS measurement.

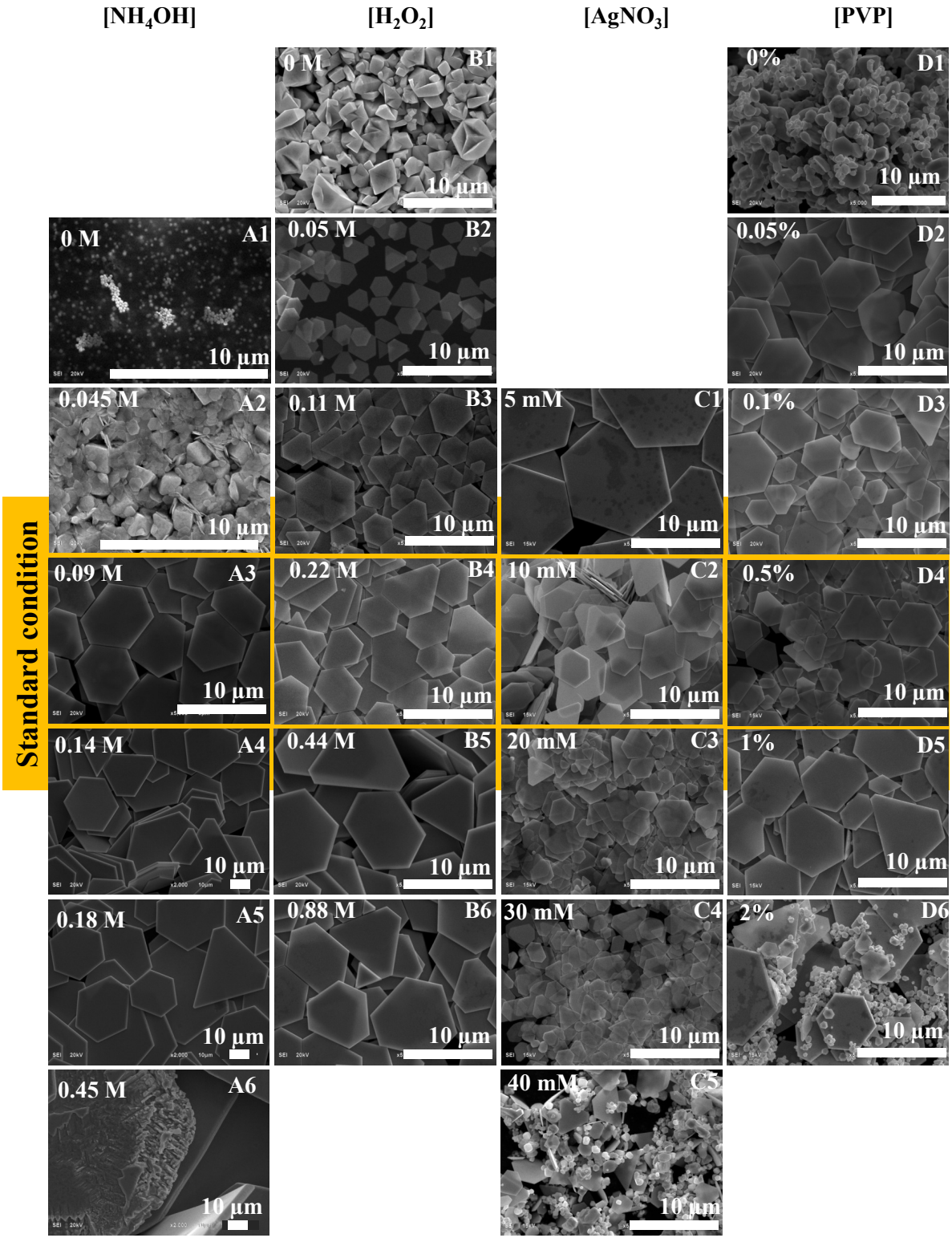

Figure S10. Expanded SEM micrographs of Figure 3 show morphological change of AgMPs induced by the experimental condition: (A) NH_4OH, (B) H_2O_2, (C) $AgNO_3$, and (D) PVP. The concentration is indicated in the figure. The scale bars indicate 10 µm.

References

1. M. Tsuji, S. Gomi, Y. Maeda, M. Matsunaga, S. Hikino, K. Uto, T. Tsuji and H. Kawazumi, *Langmuir*, 2012, **28**, 8845-8861.
2. S. H. Im, Y. T. Lee, B. Wiley and Y. Xia, *Angewandte Chemie*, 2005, **117**, 2192-2195.
3. X. Tang, M. Tsuji, P. Jiang, M. Nishio, S.-M. Jang and S.-H. Yoon, *Colloids and Surfaces A: Physicochemical and Engineering Aspects*, 2009, **338**, 33-39.
4. B. Wiley, T. Herricks, Y. Sun and Y. Xia, *Nano Letters*, 2004, **4**, 1733-1739.
5. S. Xu, B. Tang, X. Zheng, J. Zhou, J. An, X. Ning and W. Xu, *Nanotechnology*, 2009, **20**, 1-7.
6. C. M. Cobley, M. Rycenga, F. Zhou, Z.-Y. Li and Y. Xia, *The Journal of Physical Chemistry C*, 2009, **113**, 16975-16982.
7. M. J. Mulvihill, X. Y. Ling, J. Henzie and P. Yang, *Journal of the American Chemical Society*, 2009, **132**, 268-274.
8. J. Du, B. Han, Z. Liu, Y. Liu and D. J. Kang, *Crystal Growth & Design*, 2007, **7**, 900-904.
9. G. Aloisi, A. M. Funtikov and T. Will, *Journal of Electroanalytical Chemistry*, 1994, **370**, 297-300.
10. G. Beltramo and E. Santos, *Journal of Electroanalytical Chemistry*, 2003, **556**, 127-136.
11. M. L. Foresti, M. Innocenti, F. Loglio, L. Becucci and R. Guidelli, *Journal of Electroanalytical Chemistry*, 2010, **649**, 89-94.
12. B. M. Jović, V. D. Jović and D. M. Dražić, *Journal of Electroanalytical Chemistry*, 1995, **399**, 197-206.
13. K. R. Temsamani and K. Lu Cheng, *Sensors and Actuators B: Chemical*, 2001, **76**, 551-555.
14. B. V. Andryushechkin, K. N. Eltsov and V. M. Shevlyuga, *Surface Science*, 1999, **433–435**, 109-113.
15. K. J. Stevenson, X. Gao, D. W. Hatchett and H. S. White, *Journal of Electroanalytical Chemistry*, 1998, **447**, 43-51.
16. D. Aherne, D. M. Ledwith, M. Gara and J. M. Kelly, *Advanced Functional Materials*, 2008, **18**, 2005-2016.